J Fail. Anal. and Preven. (2024) 24:1906–1915
https://doi.org/10.1007/s11668-024-01979-7

ORIGINAL RESEARCH ARTICLE

Influence of Fibre Architectures on the Mechanical Properties and Damage Failures of Composite Laminates

Hussein Dalfi

Submitted: 30 September 2023 / in revised form: 17 May 2024 / Accepted: 26 June 2024 / Published online: 2 July 2024

Abstract Owing to the importance of fibre architectures in the design of textile composite materials, understanding their effect on the failure mechanisms of these composites have taken more considerations. In this regards, non-crimp preform and 2/2 twill fabric have been manufactured from glass fibre by using pin-board and power loom machines respectively, and subsequently composites laminates from both preforms are manufactured via vacuum assisted resin infusion method. In addition, quasi-static tensile and compressive strength tests have been conducted for the composite laminates that have same volume fraction. Damage failure mechanisms that occurred in compressive strength in both composites have been examined by using scanning electronic machine (SEM). Findings show that the mechanical properties are primly determined by fibre architectures and the presence of fibre crimp can further weaken tensile and compressive strength values. It was noticed that the tensile strength of non-crimp composite was 610 MPa whereas that of twill fabrics composite laminates it was found to be 350 MPa and 440 MPa in warp and weft directions respectively. Moreover, in case of twill fabric composites, fibre crimp has a considerable effect on the mode and characteristics of damage in the compressive loading; this leads to fibre fracture and kinks that primarily happened in the intersection point of warp and weft yarns. Results also showed improved ductility, strain to failure and absorbing energy in the twill fabric composites compared to non-crimp composites under in-plane shear strength test.

H. Dalfi (✉)
Mechanical Department, College of Engineering, University of Wasit, Kut, Wasit, Iraq
e-mail: hqumar@uowasit.edu.iq

Keywords Non-crimp preform · Twill fabric · Tensile and compressive tests · SEM · Composite laminates

Introduction

Two-dimensional (2D) textile composites have been widely investigated and adopted in several applications such as aerospace, aeronautics, and navy owing to their superior damage tolerance, resistance of delamination, structural integrity and tailor-ability over unidirectional laminates [1–4]. However, on account of the complex microstructure and fibre architecture, it is challenging to investigate the mechanical response of 2D woven laminates compared to UD composite laminates [5–7]. A significant factor that contributes to this complexity is fibre crimp, which has strong influence on their mechanical behaviour, mechanisms of damage, and modes of failures [8]. The 2D fabric composites have higher impact resistance and damage tolerance compared to the unidirectional and cross ply laminates [9–11]; however, their mechanical performance is lower because of the fibres interlacement and undulated region where only resin exists [12]. In this regards, researchers have paid particular attention to understand the damage mechanisms and propagation of failure modes in 2D woven composites [13–23]. Several types of fibre architectures are observed for 2D woven fabrics such as twill, satin and basket [24–26]. The effect of fibre crimp on the tensile, compressive, and flexural strength of textile composite laminates has been extensively studied by way of experimental and numerical methods [27–32]. Abot et al [33] found that the crimp value in the woven fabric reinforcement and fibre bridging have significantly affected the elastic modulus and ultimate

strength of different fabric composites. These various types of woven fabric composites had same areal density and fibre volume fraction and they were subjected to either uniaxial tensile or shear loading. Ganesh et al [34] investigated the effect of fabric pattern on the failure behaviour of plain fabric laminates under quasi-static tensile loading by adopting the two-dimensional woven composite strength model. This model has used the geometrical parameters like width, thickness and inter-gap of strand and volume fraction of fibre. It was found that the failure behaviour significantly depended on the weave geometrical parameters. Fabric composite laminates have a non-planar inter-ply structure and the resin-rich areas which can play a vital role in controlling the failure modes of fabric composite laminates i.e. delamination and crack progression [35, 36]. Ebeling et al [37] confirmed that the resin-rich areas in glass fabric composites can be classified into two types. The first one is the yarn undulation area which is formed when two yarns intersect with each other; and the depth of this area is approximately equal to half the thickness of the ply. The second type is the interstitial area which is situated at the crossing of four intersecting yarns; and the depth of this area is approximately equal to the ply thickness. Several researchers have been concentrated on the mechanical response of various woven fabric composites under compressive loading [38–40]. One of the most common failures that occurred in laminates under compressive loading is delamination. Chai et al [41] adopted a theoretical and experimental study on one-dimensional delamination buckling of composite plates using theory of beam-column delamination. They confirmed that the dimensions of the delamination, the load at which it is introduced and the fracture energy affected the buckling delamination of composite laminates. Carvalho et al [42] investigated the influence of the interlacing region of tows on the compressive failure of orthogonal 2-D woven composites with various stacking sequences. Their results, which are compared experimentally and numerically, demonstrated that the support of adjacent layers on the sequence of fabrics are considered the sources of failures on the woven composites laminates.

A numerical simulation approach based on FEM seems to be a promising and a flexible alternative which provides detailed information on the spatial and temporal evolution of elastic properties and damage failures of textile composites when they are subjected to loading [43]. Also, combining of appropriate experimental procedure with a validated FE model can lead to an accurate analysis of textile composite structures. This could provide precise understanding of the underlying deformation and damage mechanisms, and an efficient means of structural optimization. However, the development of a suitable model that can represent the physics of damage mechanisms in a textile composite is a challenging task [44]. Several research works have been focussed on prediction of elastic properties and damage failures of textile composite laminates [45, 46]. Roham Rafiee and Amirhesam Salehi [47, 48] developed multi-scale models for estimating the mechanical properties of composite layers. The modelling begins from micro-scale where spacing and contiguity of fibres are simulated. Then at the meso-scale, the effect of bundle undulation, crossovers and overlaps of fibres are captured. Finally, at the macro-scale, the distribution of stress/strain on each layer is analysed.

According to the previous study, there is lack of experimental investigation on the mechanical performances of 2D woven composites laminates. In addition, the understanding of damage failures occurring in these composites is still limited. In this regards, the damage mechanisms of two-dimensional (2D) woven composites under the quasi-static tensile, compressive and shear strength tests are examined. Scanning Electronic Microscopy (SEM) has been adopted to investigate the internal damage failures occurred in the compressive strength. With focussing on the fibre crimp, the mechanical performances of both 2D woven and non-crimp cross-ply composite laminates with same fibre volume fractions are compared.

Experimental Work

Materials and Composites preparation

In this study, the S-glass yarns with 634 tex as linear density are used to produce two types of preforms; the former is the non-crimp cross-ply and the latter is 2/2 twill fabric. The pin-board tool is adopted to create the non-crimp preforms. While the power loom machine is used to produce the 2/2 twill woven fabrics. The density of warp (end) and weft (fill), areal density, crimp value, and thickness of these preforms were determined based on the ASTM standards, i.e. D3775-02, D3776-09, D3883-04 and D1777-09, respectively, and are presented in Table 1.

In addition, the designs of preforms with TexGen software and their scanned images have been presented in Fig. 1.

Two classes of composite laminates are manufactured in this study; the first class is made with four fabric layers, while the second type is made with four 0/90 non-crimp cross-ply as shown in Fig. 2.

Epoxy resin (i.e Araldite LY 564) and its hardener (i.e. Aradur 2954) with 100:35 mixed ratio were selected as matrix to fabricate composite laminates by using method of vacuum bagging infusion. To manufacture fabric composite laminates, the fabrics are cut (250 mm × 250 mm) and stacked to produce laminates with four fabric plies.

Table 1 Specification of preforms

Preforms	Warps (cm)	Fills (cm)	Areal Density (g/m^2)	Thickness (mm)	Crimp (%) End	Crimp (%) Fill
NC- cross-ply glass	8	8	988	1.09	0	0
2/2 Twill fabric	8	8	1029	0.73(±0.02)	4.0 (±0.41)	3.5 (±0.36)

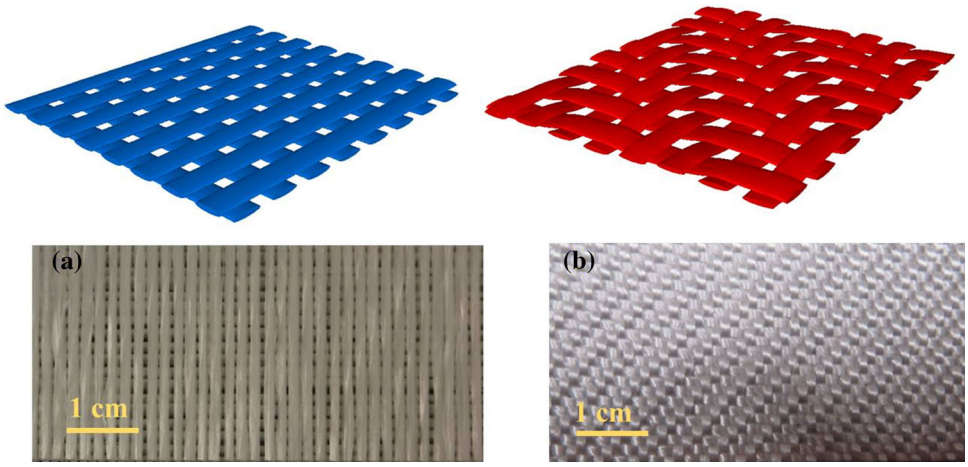

Fig. 1 Images of: (**a**) preform of non-crimp cross ply and (**b**) 2/2 twill fabric

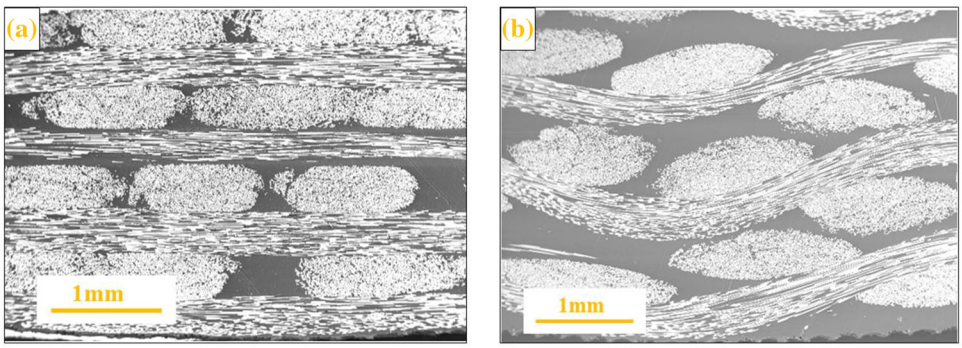

Fig. 2 The microstructure of the laminates with: (**a**) non-crimp cross ply (NO-GF) and (**b**) 2/2 twill fabric (TW-GF)

Table 2 Average properties of laminates

Code of Laminate	Vf% of S-glass	Thickness (mm)	Density (g/cm3)	Void%
NO-GF	45.00(±0.69)	3.02(±0.086)	1.76(±0.008)	1.37(±0.062)
TW-GF	45.02(±0.01)	3.40(±0.140)	1.74(±0.012)	1.32(±0.500)

While the non-crimp composite laminates are made with balanced cross-ply layup i.e. $[0/90]_4$ with eight plies representing each fabric layer with [0/90] and 500 mm × 500 mm in size. Two steps of curing are used for manufacturing these laminates; 80 °C for 120 minutes and then post-cured at 140 °C for 8 hours. Then, the laminates have been cut to the required suitable dimensions by using a diamond cutter. The details of laminates such volume fractions of glass, thickness, density and percentage of voids are illustrated in Table 2. Based on the BS EN ISO 1183-1 and BS EN ISO 1172 standards, the density and glass volume fractions are determined by using the immersion and ignition methods. Furthermore, the void percentage in the twill fabric composites is less than non-crimp composite laminates (as seen in Table 2); this is due to the effect of nesting, which leads to high compaction in the fabric composites.

The SEM micrographs are used to show the microstructure of laminates as presented in Fig. 2. The NO-GF denotes the laminates produced from non-crimp preform with S-glass yarns while the TW-GF refers to the laminates manufactured from 2/2 twill fabric with S-glass yarns. As can be seen in Fig. 2a, the composite laminate has two types of layers: warp and weft, which are

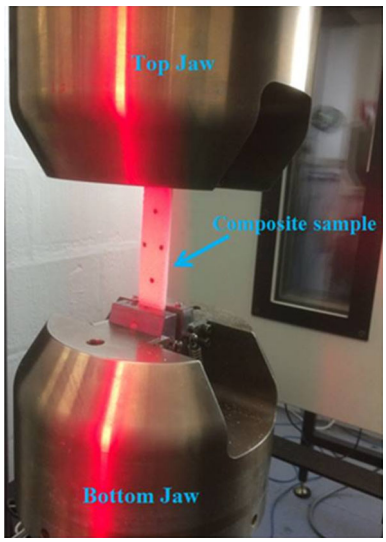

Fig. 3 Composite sample under tensile testing

practically straight and most of the fibre bundles are under good compaction. In addition, the cross-sectional shape of yarns in the weft direction is mostly lenticular and there is no resin–rich regions between plies. While the SEM images in Fig. 2b shows that the fabric layers are composed of warp and weft bundles which alternately intersect creating resin–rich regions. These intersection points are considered sources of crack initiation.

Methods of Tests

Tensile strength test

The mechanical performances such as tensile strength, modulus of elasticity, and strain to failure of all the composite samples were conducted by using tensile strength tests. Based on the ASTM D3039M 2008 standard, the samples were cut from the laminates with aiding diamond cutter to a size of 250 mm x 25 mm (length x width) and 50 mm gauge length. In each category, five specimens were prepared with tabs (made from glass composites) placed at the ends of the specimens to decrease the effect of gripping. Tensile tests were carried out by Instron 5982 universal testing machine at a crosshead rate of 2 mm/min which corresponds to a strain rate of 0.067% per second. Four dots were marked on the surface of specimen to record the strains occurred during the test by video extensometer as illustrated in Fig. 3 so that full stress/strain curves could be extracted by these strain gauges; it allowed determining the moduli and Poisson's ratio. The tensile strength (σ) and Young modulus (E) values for each sample were calculated by using the following equations:

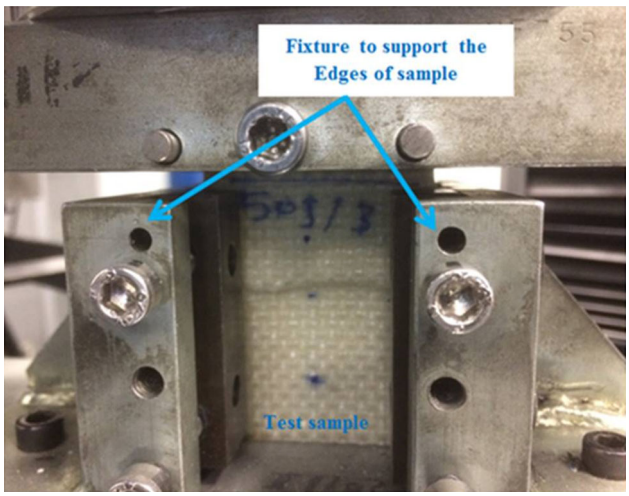

Fig. 4 Composite sample under Compressive strength test

$$\boldsymbol{\sigma} = \frac{\boldsymbol{P}}{\boldsymbol{A}} \quad \text{(Eq 1)}$$

$$\boldsymbol{E} = \frac{\boldsymbol{\sigma}_1 - \boldsymbol{\sigma}_2}{\boldsymbol{\epsilon}_1 - \boldsymbol{\epsilon}_2} \quad \text{(Eq 2)}$$

where $\boldsymbol{P}$ and $\boldsymbol{A}$ are the ultimate load and cross-sectional area of the composite sample and $\boldsymbol{\sigma}_1 - \boldsymbol{\sigma}_2$ are the tensile stresses at the strain $\boldsymbol{\epsilon}_1 = 0.0025$ and $\boldsymbol{\epsilon}_2 = 0.0005$ respectively.

Compressive Strength Test

In order to study the influence of fibre architecture on the compressive strength of composite laminates, the compressive strength tests were adopted by using Instron 5989 test machine at room temperature with 300 kN loading capacity and 0.5 mm/min constant displacement. The samples have been cut with dimensions as 89 mm × 55 mm (length and width respectively) based on the Pichard and Hogg protocol for impact and CAI tests [49]. In addition, the edges of these samples were supported by fixture to avoid buckling as presented in Fig. 4.

Compression strength of the laminates is determined when the laminates reach their maximum failure force as described by the following equation:

$$\boldsymbol{\sigma_c} = \frac{\boldsymbol{F_{max}}}{\boldsymbol{w.t}} \quad \text{(Eq 3)}$$

where $\boldsymbol{\sigma_c}$ is ultimate compressive strength MPa; $\boldsymbol{w}$ is specimen width (mm); $\boldsymbol{t}$ is the specimen thickness (mm);$\boldsymbol{F_{max}}$ is the maximum failure prior the failure (N).

In-plane Shear Strength Test

In order to investigate the shear strength properties of composite laminates, the in-plane shear strength test was

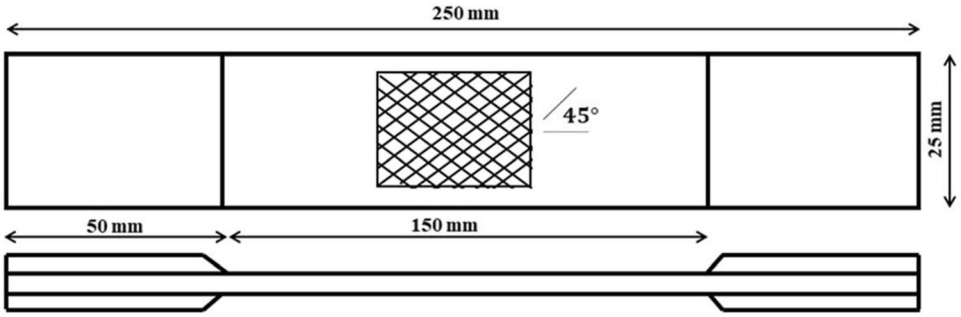

Fig. 5 Dimensions of sample in-plane shear test

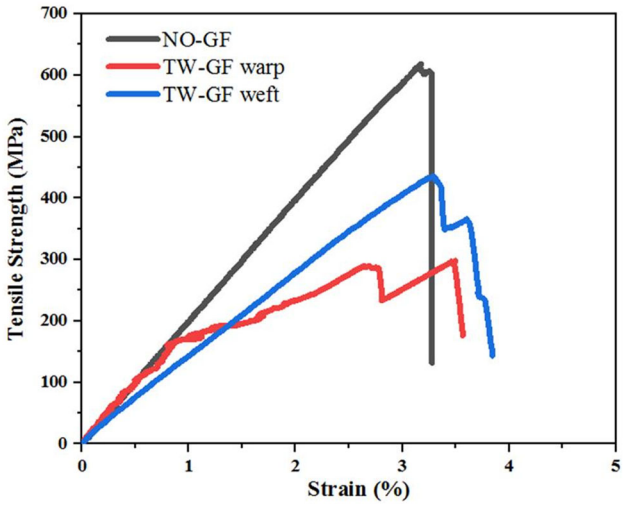

Fig. 6 Tensile strength- strain curves of all laminates

conducted according to the standard ASTM D3518M − 13 [22]. The specimen dimensions were set as 250 mm × 25 mm (length and width respectively) as shown in the Fig. 5. And all the shear tests were done at room temperature with a crosshead rate of 2 mm/min using the same universal testing machine utilised in the tensile tests. The shear strength (τ) and shear strain (γ) were calculated using the following equations:

$$\tau = \frac{P}{2wt} \quad \text{(Eq 4)}$$

$$\gamma = \epsilon_{xx} - \epsilon_{yy} \quad \text{(Eq 5)}$$

where $P, w, t,$ are load, width and thickness of sample respectively; $\epsilon_{xx} and \epsilon_{yy}$ are strains in both longitudinal and transverse directions. The slope of shear-strain curve at 0.5% is adopted to calculate the shear modulus as following:

$$G = \frac{Shear\ stress}{shear\ starin} \quad \text{(Eq 6)}$$

Damage Characterisation

In this study, the failure mechanisms that occurred in samples due to the compressive strength tests have been examined by using Scanning Electron Microscope (SEM). These investigations were done by Philips model XL 30 field emission gun (FEG) microscope. Further, a precision cutter was used to cut the samples and then these samples were coated with thin layer of carbon by Quorum Q150T ES machine to improve their conductivity to avoid the accumulation of charges.

Results and Discussion

Tensile Strength Test Results

Figures 6 and 7 showed the tensile properties of non-crimp and twill fabric in warp and weft directions composite laminates versus stress-strain response, tensile strength, moduli and strain to failure for all laminates. As can be seen in Fig. 6, there are instant drops after peaks for all plots profile; this indicates that the catastrophic failure can occur due to the fibre fractures. Edgren et al [50] have confirmed that by increasing the load, the linear behaviour of the stress-strain curve of non-crimp glass composites was changed to non-linear; and this is due to the first damage which happened as transverse matrix cracks (i.e. half cracks and longitudinal crack in the 90 plies). These cracks with slightly higher strain developed into double cracks followed by delamination between 0/90 interface.

The curve profile of twill fabric composites in both warp and weft directions showed nonlinearity behaviour compared to non-crimp composite laminates owing to fibre undulation. Unlike the curve profile of non-crimp, the twill fabric composite presented long tails and illustrated ductile behaviour and this can be attributed to the crimp of yarns. Comparing the previous work, Rios-Soberanis et al [51] showed that the intersection point between warp and weft (i.e. crimp) in woven fabric composite is considered as the

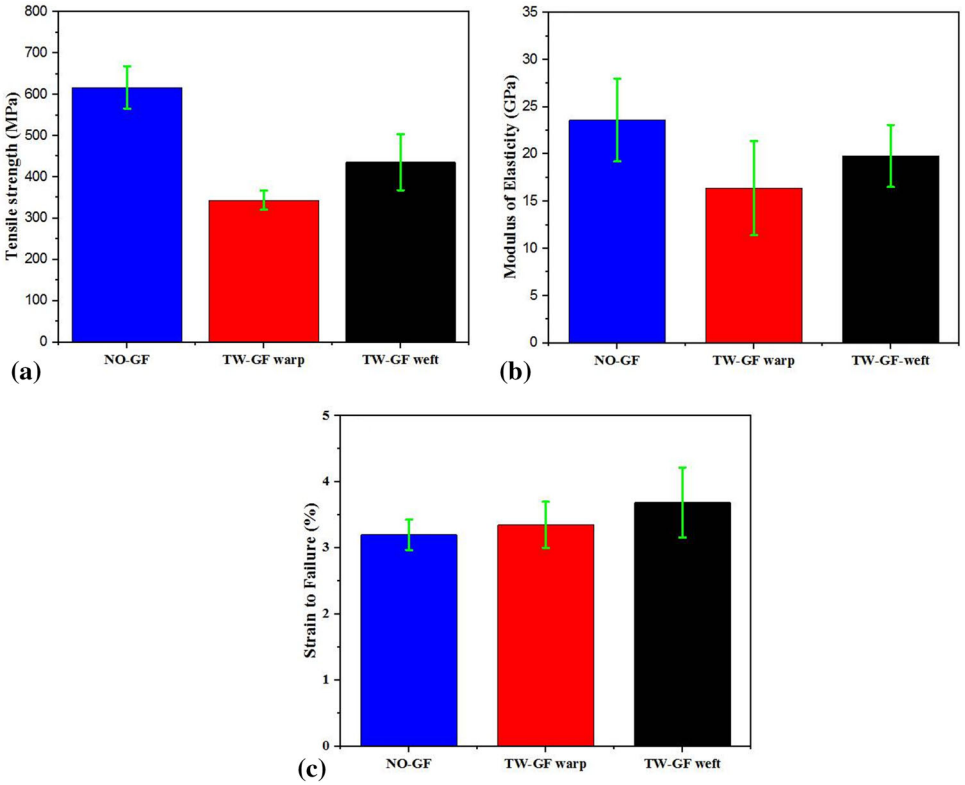

Fig. 7 The laminates properties: (**a**) tensile strength, (**b**) modulus of elasticity, and (**c**) strain to failure

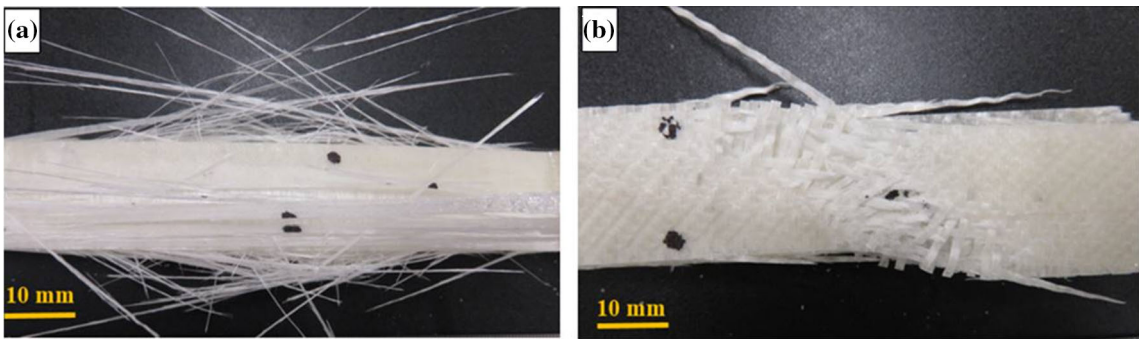

Fig. 8 A typical tensile damage region of (**a**) Non-crimp and (**b**) twill fabric composite laminates

weakest region during load application and it is attributed to the concentration of the stresses matrix.

Moreover, it can be seen in Fig. 6 that the moduli and strength values of twill fabrics composites in both directions are approximately half of that of the non-crimp composite laminates and the undulation of yarns in the warp and weft direction is considered a main reason compared to the straight yarns in the non-crimp composite laminates.

Figure 8 illustrates the top view of typical tensile damage failure for non-crimp and twill fabric laminates. As can be noticed in Fig. 8a, the major tensile damage mode for non-crimp composite is fibre breakage. Further, interlayer debonding produced by stress release causes accompanying transvers splitting. In this regards, the dominant tensile failure can be observed in the direction normal to the nearly flat fracture plane. *Aymerich and Priolo* [52] have another opinion on the damage failures in cross-ply composites. They manufactured cross-ply graphite composite laminates (0°/90°). Their findings confirmed that the initial damage consisted of tensile matrix crack in the lowest 0° plies followed by shear matrix cracking in the 90° plies and delamination mainly affecting the distal (90°/0°) interface. Furthermore, the fibre breakage is visible in the surface layer of damaged composite laminates.

Unlike non-crimp composite laminate, the major load-bearing yarn in case of twill fabric composite is undulated.

Table 3 Compression strength properties of laminates

Code of Laminates	Compressive strength (MPa)	Compressive modulus (GPa)	Strain to Failure
NO-GF	276 (±16.19)	17.00(±0.31)	0.021 (±0.008)
TW-GF	140 (±0.01)	12.01(±0.23)	0.011 (±0.012)

This undulated sinusoidal shape of warp leads to a highly risky fibre fracture region that can be concentrated at the intersection points between warp and weft yarns as illustrated in Fig. 8b. Therefore, the fracture plane of twill fabric composite is inclined and the inter-yarns debonding is curved which follows the outlines of weft yarns.

Compressive Strength Test Results

The compression strength properties of composite laminates have been shown in Table 3. Figure 9 presents the representative compressive stress versus strain for composite laminates. It was seen that at the initial stage, the compressive stress raised slowly as all clearances between fixture and specimen are being eliminated. After clearance elimination, there was a continuous linear increment in applied stress with strain. After the compressive stress reached certain values, the load was dropped suddenly and this is because of the failure load of the specimen.

Figure 10 presented the compressive damage failures and their region in picture of non-crimp cross ply and twill fabric laminates. It can be seen in Fig. 10a that the major compressive damage modes in the non-crimp cross ply laminates are the fibre kinking formation resulting buckling which produced intra-layer and inter-layer debonding and they are spreading to create delamination. Whereas, the kinking zone in twill fabric laminates can be observed at the intersection points between warp and weft yarns as shown in Fig. 10b. This illustrates the influence of fibre architecture on the creation kink bands.

In-plane Shear Test Results

Comparative plots of shear stress-shear strain for non-crimp glass and twill glass fabric composite laminates are shown in Fig. 11 and the mechanical characterisation of these composites' curves are presented in Table 4. It can be noticed in Fig. 11 that the NO-GF samples experienced a rapid and steep rise in stress up to a maximum stress of 98 MPa followed by immediate rupture and catastrophic failure and this is because of the high strength properties of glass fibre. In contrast, a different trend can be seen in the TW-GF samples, which illustrated a gradual decrease in the tensile stress (56 MPa); the samples became less stiff and resisted the tensile loading in a ductile manner owing

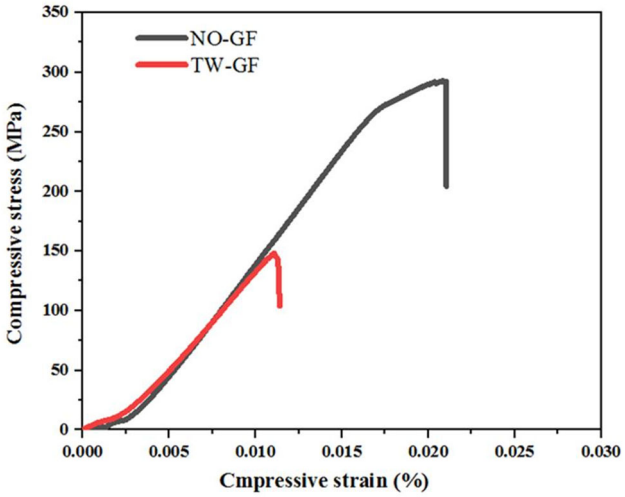

Fig. 9 Representative compress stress-strain plots of laminates

to the fibre crimp. The knee point, which indicated the change in the stress-strain slope, also depended on the fibre architecture of the composites. It can be seen that the linear behaviour of the stress-strain curve of NO-GF samples changed to non-linear at 1.5 % strain with increasing the load. This outcome is due to the initial damage which occurred in the form of transverse matrix cracks (i.e. half cracks and longitudinal crack in the 90° plies). Under marginally higher strain, these cracks developed to form double cracks followed by delamination between the 0/90 interface. Meanwhile, the findings from the TW-GF samples yielded a lower knee point at 1% strain level and short phases in the elastic behaviour were observed; this is due to the higher numbers of interstitial positions and more resin rich regions which are considered to be related to the crimp and the waviness of the longitudinal yarns.

The weight specific energy absorption (SEA) of composite samples in the shear strength test has been measured from integration area under shear stress-strain curve divided by density of composite sample according to the following equation:

$$\boldsymbol{SEA} = \frac{1}{\boldsymbol{\rho}} \int \boldsymbol{\sigma}(\epsilon) \boldsymbol{d\epsilon} \qquad \text{(Eq 7)}$$

where $\rho, \sigma, and \epsilon$ are density, stress and strain respectively.

From Fig. 12, it can be seen that the SEA depends on the evaluated mechanical properties of composite samples and their densities presents a remarkable fibre architecture dependency. The higher value of SEA in TW-GF samples can be attributed to the fibre crimp which produced ductile manner failure leading to higher strain failure compared to the NO-GF samples. In comparison to the previous work, *Tim Bergmannet et al* [53] confirmed that the strain to failure and absorbed energy increased in the textiles

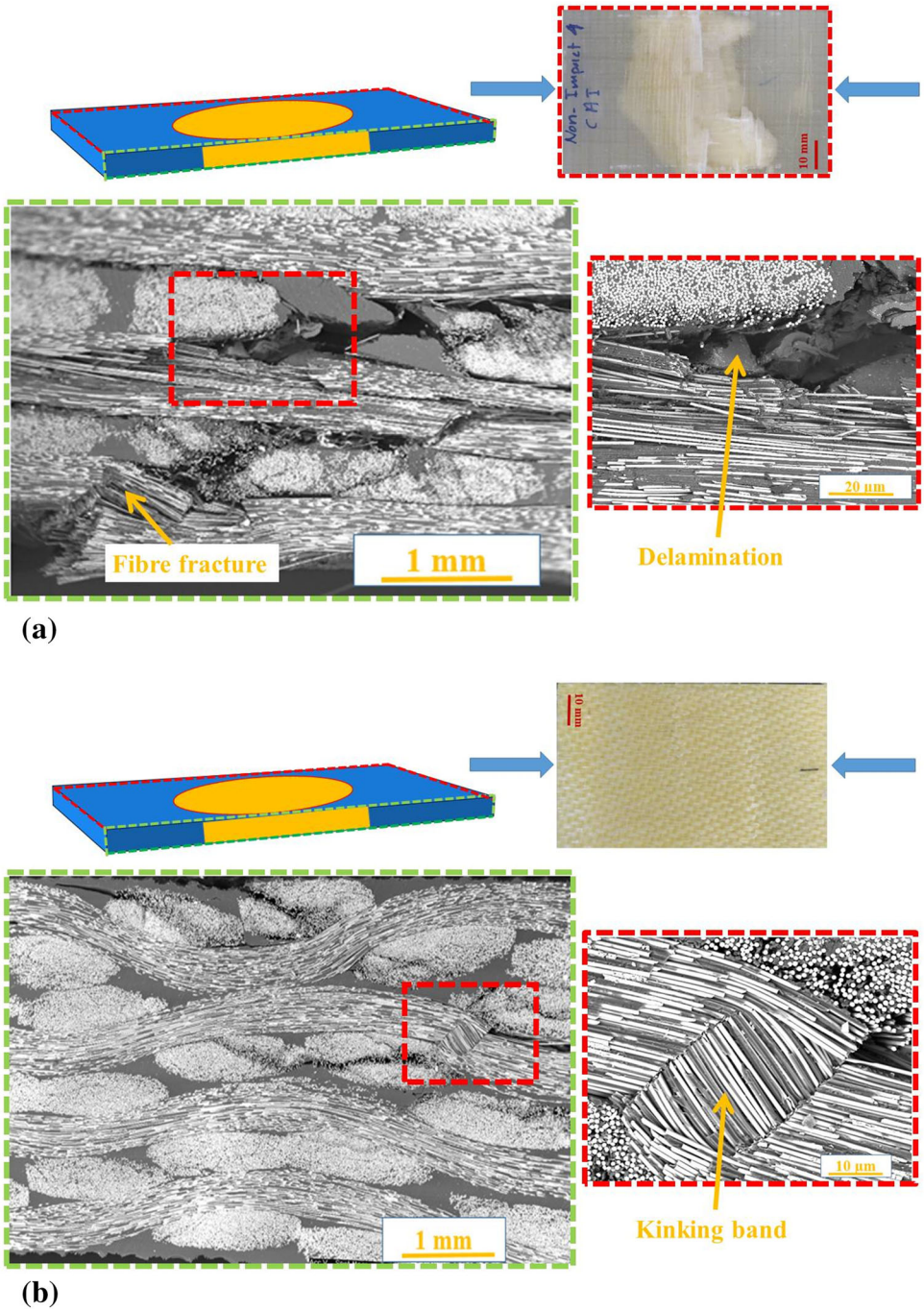

Fig. 10 Typical damage failure modes of (**a**) Non-crimp composite laminates and (**b**) Twill fabric composite laminates

composites that have higher value of fibre crimp such as 2/2 twill composite when subjected to in-plane shear strength tests.

Conclusions

In this research work, the influence of fibre architecture on quasi-static tensile, compressive and shear performances of laminates has been investigated. Non-crimp preform and twill fabric laminates produced from glass fibres have been used to develop composite laminates using vacuum bagging method. Tensile, compressive and in-plane shear strength tests are used to evaluate the mechanical properties (i.e. Tensile, compressive, and shear strengths), while the damage mechanisms induced by fibre architectures were analysed and studied by using SEM machine. Findings show that the fibre crimp in twill fabric laminates not only weakens the mechanical performances but also influences on the damage failures modes and

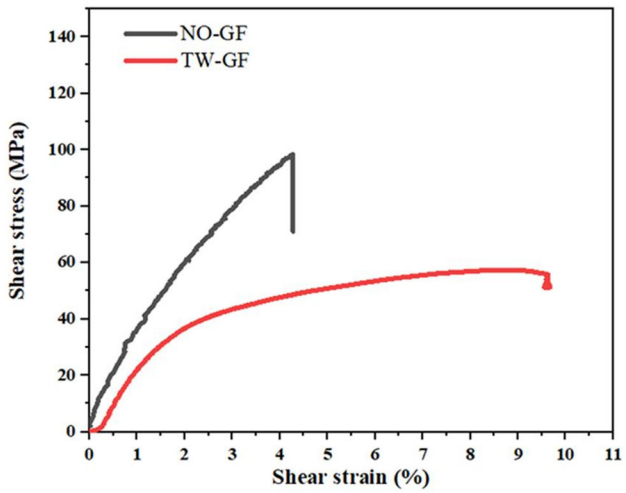

Fig. 11 Shear stress-strain curves for composite laminates

Table 4 Shear strength properties of laminates

Code of Laminates	Shear strength (MPa)	Shear modulus (GPa)	Strain to Failure
NO-GF	98.30 (±0.75)	10.35 (± 1.50)	4.30 (±0.21)
TW-GF	56.12 (±1.60)	3.70 (±0.21)	9.65 (±1.37)

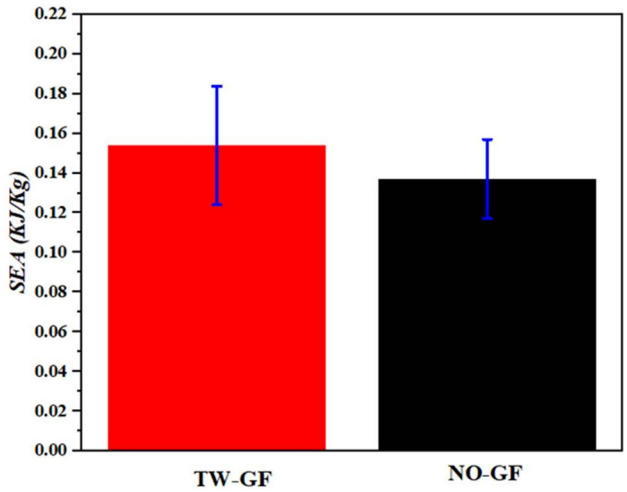

Fig. 12 The weight specific energy absorption (SEA) of composite samples

characteristics. It was noticed that the tensile strength of twill fabric composite laminates in warp and weft directions are 350 MPa and 440 MPa compared to 610 MPa in the non-crimp composite laminates. Moreover, the fibre crimp in the twill fabric composites has substantial effect on these mechanisms in terms of damage location of fibre fracture and inter-layer debonding pathways. The results also show that the strain to failure, absorbed energy and ductility improved in twill fabric composites compared to the non-crimp composite laminates due to the effect of fibre crimp. The fibre fracture and kinks region often occurred at the intersection points between warp and weft yarns. These views into the influence of fibre architecture into damage mechanisms can be considered guidance for the optimum design of textile composite materials.

Author contributions Hussein Dalfi contributed to Conceptualization, Methodology, Investigation, Original draft preparation, Writing –review & editing of paper.

Funding The author(s) received no financial support for the research, authorship, and/or publication of this article.

Conflict of interest The author(s) declared no potential conflicts of interest with respect to the research, authorship, and/or publication of this article.

References

1. G. Ernst, M. Vogler, C. Hühne, R. Rolfes, Multiscale progressive failure analysis of textile composites. Compos. Sci. Technol. **70**(1), 61–72 (2010)
2. Y. Li et al., A review of high-velocity impact on fiber-reinforced textile composites: potential for aero engine applications. Int. J. Mech. Syst. Dyn. **2**(1), 50–64 (2022)
3. M. Ansar, W. Xinwei, Z. Chouwei, Modeling strategies of 3D woven composites: A review. Compos. Struct. **93**(8), 1947–1963 (2011)
4. R. Rolfes, G. Ernst, D. Hartung, and J. Teßmer, "Strength of textile composites–A voxel based continuum damage mechanics approach," *Computational mechanics-solids, structures and coupled problems,* pp. 497-520, 2006.
5. W. Zhou et al., A comparative study of a quasi 3D woven composite with UD and 2D woven laminates. Compos. A Appl. Sci. Manuf. **139**, 106139 (2020)
6. A. Mouritz, B. Cox, A mechanistic interpretation of the comparative in-plane mechanical properties of 3D woven, stitched and pinned composites. Compos. A Appl. Sci. Manuf. **41**(6), 709–728 (2010)
7. H.K. Dalfi, M. Tausif, Z. Yousaf, Effect of twist level on the mechanical performance of S-glass yarns and non-crimp cross-ply composites. J. Ind. Text. **51**(2_suppl), 2921–2943 (2022)
8. X. Liu, K. Rouf, B. Peng, W. Yu, Two-step homogenization of textile composites using mechanics of structure genome. Compos. Struct. **171**, 252–262 (2017)
9. J.-K. Kim, M.-L. Sham, Impact and delamination failure of woven-fabric composites. Compos. Sci. Technol. **60**(5), 745–761 (2000)
10. M.V. Hosur, M. Adbullah, S. Jeelani, Studies on the low-velocity impact response of woven hybrid composites. Compos. Struct. **67**(3), 253–262 (2005)
11. P. Curtis, S.J.C. Bishop, An assessment of the potential of woven carbon fibre-reinforced plastics for high performance applications. Composites. **15**(4), 259–265 (1984)
12. J.N. Baucom, M.A. Zikry, Low-velocity impact damage progression in woven E-glass composite systems. Compos. Part A Appl. Sci. Manuf. **36**(5), 658–664 (2005)
13. Z. Ming Huang, The mechanical properties of composites reinforced with woven and braided fabrics. Compos. Sci. Technol. **60**(4), 479–498 (2000)

14. J. Byström, N. Jekabsons, J. Varna, An evaluation of different models for prediction of elastic properties of woven composites. Compos. B Eng. **31**(1), 7–20 (2000)
15. J. Whitcomb, K. Woo, Enhanced direct stiffness method for finite element analysis of textile composites. Compos. Struct. **28**(4), 385–390 (1994)
16. K. Katnam, H. Dalfi, P. Potluri, Towards balancing in-plane mechanical properties and impact damage tolerance of composite laminates using quasi-UD woven fabrics with hybrid warp yarns. Compos. Struct. **225**, 111083 (2019)
17. H. Dalfi, K.B. Katnam, P. Potluri, Intra-laminar toughening mechanisms to enhance impact damage tolerance of 2D woven composite laminates via yarn-level fiber hybridization and fiber architecture. Polym. Compos. **40**(12), 4573–4587 (2019)
18. H. Dalfi, K. Babu-Katnum, P. Potluri, E. Selver, The role of hybridisation and fibre architecture on the post-impact flexural behaviour of composite laminates. J. Compos. Mater. **55**(11), 1499–1515 (2021)
19. H. Dalfi, Effect of intra-yarn hybridisation and fibre architecture on the impact response of composite laminates: Experimental and numerical analysis. Proc. Inst. Mech. Eng. C J. Mech. Eng. Sci. **236**(6), 3004–3026 (2022)
20. H. Dalfi, Improving the mechanical performance and impact damage tolerance of glass composite laminates via multi-scales of hybridisation. Proc. Inst. Mech. Eng. Part L J. Mater. Des. Appl. **236**(12), 2339–2356 (2022)
21. H. Dalfi, A.J. Al-Obaidi, H. Razaq, The influence of the inter-ply hybridisation on the mechanical performance of composite laminates: Experimental and numerical analysis. Sci. Prog. **104**(2), 00368504211023285 (2021)
22. H.K. Dalfi, A. Al-Obaidi, E. Selver, Z. Yousaf, P. Potluri, Influence of yarn-hybridisation on the mechanical performance and thermal conductivity of composite laminates. J. Ind. Text. **51**(3_suppl), 5086S-5112S (2022)
23. H.K. Dalfi, Z. Yousaf, E. Selver, P. Potluri, Influence of yarn hybridisation and fibre architecture on the compaction response of woven fabric preforms during composite manufacturing. J. Ind. Text. **51**(3), 5062S-5085S (2022)
24. S. Adanur, *Handbook of weaving*. (CRC Press, 2020)
25. B. N. Cox, G. Flanagan, Handbook of analytical methods for textile composites. (1997)
26. M. Mariatti, M. Nasir, H. Ismail, Influence of different woven geometry and ply effect in woven thermoplastic composite behaviour-Part 2. Int. J. Polym. Mater. **47**(2–3), 499–512 (2000)
27. T. Osada, A. Nakai, H. Hamada, Initial fracture behavior of satin woven fabric composites. Compos. Struct. **61**(4), 333–339 (2003)
28. X. Tang, J.D. Whitcomb, Progressive failure behaviors of 2D woven composites. J. Compos. Mater. **37**(14), 1239–1259 (2003)
29. T. Ishikawa, T.-W. Chou, Stiffness and strength behaviour of woven fabric composites. J. Mater. Sci. **17**, 3211–3220 (1982)
30. N. Naik, P. Shembekar, Elastic behavior of woven fabric composites: I—Lamina analysis. J. Compos. Mater. **26**(15), 2196–2225 (1992)
31. J.D. Whitcomb, Three-dimensional stress analysis of plain weave composites. Compos. Mater. Fatigue Fract. **3**, 417–438 (1991)
32. M.G. Kollegal, S. Sridharan, Strength prediction of plain woven fabrics. J. Compos. Mater. **34**(3), 240–257 (2000)
33. J.L. Abot, R.D. Gabbai, K. Harsley, Effect of woven fabric architecture on interlaminar mechanical response of composite materials: an experimental study. J. Reinf. Plast. Compos. **30**(24), 2003–2014 (2011)
34. V. Ganesh, N. Naik, Failure behavior of plain weave fabric laminates under on-axis umnaxial tensile loading: III—Effect of fabric geometry. J. Compos. Mater. **30**(16), 1823–1856 (1996)
35. E. Greenhalgh, M. Hiley, *Fractography of polymer composites: current status and future issues*. (CRC Press, 2008)
36. Y. Siow, V. Shim, An experimental study of low velocity impact damage in woven fiber composites. J. Compos. Mater. **32**(12), 1178–1202 (1998)
37. T. Ebeling, A. Hiltner, E. Baer, I. Fraser, M. Orton, Delamination failure of a woven glass fiber composite. J. Compos. Mater. **31**(13), 1318–1333 (1997)
38. H. Chai, C.D. Babcock, Two-dimensional modelling of compressive failure in delaminated laminates. J. Compos. Mater. **19**(1), 67–98 (1985)
39. S. Wang, N. Zahlan, H. Suemasu, Compressive stability of delaminated random short-fiber composites, part I—modeling and methods of analysis. J. Compos. Mater. **19**(4), 296–316 (1985)
40. S.V. Chikkol, P.K.P. Wooday, S.J. Yelaburgi, Buckling of laminated composite cylindrical skew panels. J. Thermoplast. Compos. Mater. **30**(9), 1175–1199 (2017)
41. H. Chai, C.D. Babcock, W.G. Knauss, One dimensional modelling of failure in laminated plates by delamination buckling. Int. J. Solids Struct. **17**(11), 1069–1083 (1981)
42. N. De Carvalho, S. Pinho, P. Robinson, An experimental study of failure initiation and propagation in 2D woven composites under compression. Compos. Sci. Technol. **71**(10), 1316–1325 (2011)
43. M. Schwab, M. Todt, M. Wolfahrt, H. Pettermann, Failure mechanism based modelling of impact on fabric reinforced composite laminates based on shell elements. Compos. Sci. Technol. **128**, 131–137 (2016)
44. F. Van Der Meer, L. Sluys, Continuum models for the analysis of progressive failure in composite laminates. J. Compos. Mater. **43**(20), 2131–2156 (2009)
45. A. Tasdemirci, G. Tunusoglu, M. Güden, The effect of the interlayer on the ballistic performance of ceramic/composite armors: Experimental and numerical study. Int. J. Impact Eng. **44**, 1–9 (2012)
46. P. Manikandan, G.B. Chai, A layer-wise behavioral study of metal based interply hybrid composites under low velocity impact load. Compos. Struct. **117**, 17–31 (2014)
47. R. Rafiee, A. Salehi, A novel recursive multi-scale modeling for predicting the burst pressure of filament wound composite pressure vessels. Appl. Phys. A. **128**(5), 388 (2022)
48. R. Rafiee, A. Salehi, Estimating the burst pressure of a filament wound composite pressure vessel using two-scale and multi-scale analyses. Mech. Adv. Mater. Struct. **30**(13), 2668–2683 (2023)
49. J.C. Prichard, P. Hogg, The role of impact damage in post-impact compression testing. Composites. **21**(6), 503–511 (1990)
50. F. Edgren, D. Mattsson, L.E. Asp, J.J.C.S. Varna, Formation of damage and its effects on non-crimp fabric reinforced composites loaded in tension. Compos. Sci. Technol. **64**(5), 675–692 (2004)
51. C.R. Rios-Soberanis, R.H. Cruz-Estrada, J. Rodriguez-Laviada, E.J.D. Perez-Pacheco, Study of mechanical behavior of textile reinforced composite materials. Dyna. **79**(176), 115–123 (2012)
52. F. Aymerich, P. Priolo, Characterization of fracture modes in stitched and unstitched cross-ply laminates subjected to low-velocity impact and compression after impact loading. Int. J. Impact Eng. **35**(7), 591–608 (2008)
53. T. Bergmann, S. Heimbs, M. Maier, Mechanical properties and energy absorption capability of woven fabric composites under±45 off-axis tension. Compos. Struct. **125**, 362–373 (2015)